

Bearing Capacity of Square and Circular Footings on a Finite Layer of Granular Soil Underlain by a Rigid Base

A. B. Cerato, A.M.ASCE¹; and A. J. Lutenecker, P.E., M.ASCE²

Abstract: Traditional bearing capacity theories for the ultimate capacity of shallow foundations assume that the thickness of the bearing stratum is infinite. The presence of a hard layer within a certain depth below the foundation can significantly influence the unit load supported by the soil. Therefore the original bearing capacity equations should be modified to account for this condition in determining the ultimate bearing capacity. In order to evaluate this phenomenon further, model square and circular footing tests were performed on a bed of well-graded sand. Test beds were prepared at three different relative densities corresponding to loose, medium, and dense conditions: $D_r=24, 57,$ and 87% , using five different sand layer thicknesses, H ; H/B values of 0.5, 1, 2, 3, and 4, where B is the footing width. Results of the model scale footing tests show that the bearing capacity factor, N_γ , should be modified up to $H/B=3$, instead of $H/B=1$, as previously suggested. The footing shape factor, s_γ , should account for both shape and finite layering. This technical note gives a description of the test methods and material used and presents the test results in comparison to previous results.

DOI: 10.1061/(ASCE)1090-0241(2006)132:11(1496)

CE Database subject headings: Scale effect; Bearing capacity; Spread foundations; Sand; Layered soils; Shape.

Introduction

It has been shown that for shallow foundations, the presence of a rigid boundary within the zone of soil developing bearing capacity increases the unit load supported by the soil. This occurs provided the boundary exists within a certain depth beneath the base of the footing. Experimental and theoretical results previously presented in the literature have suggested that if this boundary is located within a zone less than about $1.5-2 B$ ($H/B=1.5-2$) beneath the footing, depending on the sand type and relative density, the effect of the rigid boundary is to increase the bearing capacity.

Currently, both the bearing capacity factor, N_γ , and the footing shape factor, s_γ , are modified for footings resting on zone of soil overlying a rigid boundary with a thickness of soil to footing width ratio, $H/B \leq 1$. From the results obtained in this study with square and circular footings on well-graded glacial sand, it is shown that the modification of both factors should extend to $H/B \leq 3$. The shape factors should consider the H/B rigid bound-

ary and friction angle and also account for shape; i.e., square and circular footings give different ultimate bearing capacity values. Terzaghi's (1943) shape factors for square and circular footings should be used to account for differences in capacity regardless of finite layering and N_γ^* should be further modified to $H/B \leq 3$ to reflect the influence of a rigid base on ultimate bearing capacity.

Background

Modified Bearing Capacity Factors for Rigid Layers

The traditional bearing capacity equation for a surface strip footing resting on a cohesionless granular soil with zero cohesion can be stated as

$$q_{ult} = 0.5\gamma BN_\gamma \quad (1)$$

where q_{ult} =ultimate capacity of footing (kN/m^2); B =footing width (m); γ =soil unit weight (kN/m^3); and N_γ =bearing capacity factor.

When the layer between the footing and the rigid base, H , is sufficiently thin the bearing capacity factor, N_γ , should be modified to N_γ^* .

Mandel and Salencon (1972) developed a solution for the modified bearing capacity factor, N_γ^* , using the theory of limit equilibrium as a function of the friction angle, ϕ' , and H/B . Mandel and Salencon (1972) found that for $H/B \geq 1$ the value of N_γ^* was equal to N_γ . Mandel and Salencon's (1972) investigation showed that for $H/B \leq 1$ a modification of the general bearing capacity factor was necessary because the rough rigid base interfered with the slip lines and produced a considerably higher ultimate bearing capacity.

¹Assistant Professor, Dept. of Civil Engineering and Environmental Science, Univ. of Oklahoma, Norman, OK 73019 (corresponding author). E-mail: acerato@ou.edu

²Professor and Head, Dept. of Civil and Environmental Engineering, Univ. of Massachusetts, Amherst, MA 01003. E-mail: lutenegg@ecs.umass.edu

Note. Discussion open until April 1, 2007. Separate discussions must be submitted for individual papers. To extend the closing date by one month, a written request must be filed with the ASCE Managing Editor. The manuscript for this technical note was submitted for review and possible publication on March 18, 2005; approved on April 28, 2006. This technical note is part of the *Journal of Geotechnical and Geoenvironmental Engineering*, Vol. 132, No. 11, November 1, 2006. ©ASCE, ISSN 1090-0241/2006/11-1496-1501/\$25.00.

Table 1. Summary of Previous Results of Footing Tests on Limited Layer of Sand

Reference	Footing shape	Friction angle, ϕ' (degrees) ^a	Relative density D_r (%)	Width/diameter (m)	D_{50} (mm)	H/B range	N_γ^* range
Narahari and Singh (1964)	Square	44 ^b	—	0.076	0.2	0.33–3	1,437–292
Meyerhof (1974)	Circular	38 ^b	—	0.076	—	0.25–2.1	1,350–64
Tournier and Milovic (1977)	Square	38 ^a	66	0.20	0.1–0.6	0.5–6.8	508–151
	Square	38 ^a	66	0.35	0.1–0.6	0.5–6.8	245–128
	Square	38 ^a	66	0.50	0.1–0.6	0.5–6.8	134–96
Pfeifle and Das (1979)	Square	43 ^a	78	0.051	0.6	0.4–5.0	1,002–210
Hanna (1981)	Circular	43 ^b	47	0.05	—	0–2	207–59
Siraj-Eldine and Bottero (1987)	Circular	35 ^b	71	0.05	0.7	0.5–2.1	824–117
	Circular	35 ^b	71	0.056	0.7	0.5–2.2	784–111
	Square	35 ^b	71	0.05	0.7	0.5–2.0	780–121
Cooke (1988)	Circular	37 ^b	30	0.305	0.2	0.5–3.0	192–48
	Circular	44 ^b	44	0.305	0.2	0.5–3.1	2,002–200

^aTriaxial compressions.^bDirect shear box.

Modified Shape Factors for Rigid Layer

In addition to the modification of the bearing capacity factor, N_γ to N_γ^* , to account for a rigid boundary layer, Meyerhof (1974) found that the shape factor, s_γ , was also affected by a rigid layer and proposed a modified shape factor, s_γ^* , for circular foundations for a rigid boundary within a depth of $H/B \leq 1$. Meyerhof (1974) used Mandel and Salencon's (1972) analyses to develop a modified shape factor chart as a function of H/B and ϕ' for $H/B \leq 1$. Since Meyerhof's theory was based on $N_\gamma^* = N_\gamma$ at $H/B \geq 1$, the shape factor for circular footings remains constant at 0.6 for any $H/B \geq 1$.

Meyerhof (1974) modified his solution for circular footing shape factors to accommodate square and rectangular footings with the equation

$$s_{\gamma(\text{square})}^* = \left\{ 1 - \left[1 - s_{\gamma(\text{circle})}^* \right] \frac{B}{L} \right\} \quad (2)$$

Because B/L for a square footing is equal to 1, Eq. (2) gives the same s_γ^* value for square and circular footings. This varies from Terzaghi's (1943) theory, which suggests that for an infinite layer, square and circular footings should have different shape factors; i.e., Terzaghi (1943) implicitly suggested shape factors, $s_\gamma = 0.8$ and 0.6 , for square and circular foundations, respectively. This modified shape factor, s_γ^* , is an additional term in Terzaghi's (1943) original bearing capacity equation, which was for strip footings, where $s_\gamma = 1$

$$q_{\text{ult}} = 0.5\gamma BN_\gamma s_\gamma \quad \text{or} \quad 0.5\gamma BN_\gamma^* s_\gamma^* \quad (3)$$

Unlike Meyerhof's (1974) theory which suggests that s_γ^* is affected by rigid boundaries, both the bearing capacity factor and the shape factor presented by Terzaghi (1943) assume no interference within the zone of soil contributing to bearing capacity that might be produced by a layer of limited thickness.

Variation in Bearing Capacity Factor with H/B

A number of experimental 1-g investigations have been conducted to evaluate the effect of a finite layer on the bearing capacity factor N_γ . These investigations are summarized in Table 1. Most of the tests were performed on dense sands with ϕ ranging

from 35 to 44°. The value of q_{ult} was defined as the peak load in Narahari and Singh's (1964) work; however, in the remaining six experimental studies the method for determining q_{ult} was not reported. N_γ^* was backcalculated from the published ultimate capacity load test results using Eq. (3), where values of s_γ^* values were determined using Meyerhof's (1974) definition.

Investigation

In order to evaluate the current modification practices of N_γ^* and s_γ^* to account for the influence of a rigid base, model square and circular footing tests were performed on a sand layer of finite thickness. Model tests were performed in a test box ($B \leq 0.102$ m). The larger model footing tests with widths and diameters of the footings ranging from $B = 0.152$ to 0.457 m were performed in a sand pit.

Several sand characterization tests were performed on the winter sand, including specific gravity, maximum and minimum density, grain size, and two-dimensional (2D) image analysis. The results of these tests are presented in Table 2. Knowing the average sand shape helps explain shear strength tendencies whether

Table 2. Winter Sand Characteristics

G	(Mg/m ³)	2.69
ρ_{min}	(Mg/m ³)	1.61
ρ_{max}	(Mg/m ³)	1.96
e_{min}	—	0.37
e_{max}	—	0.67
D_{10}	(mm)	0.2
D_{50}	(mm)	0.7
C_c	—	1.0
C_u	—	4.5
Fines (%)	—	2.5
Form factor	($4\pi A/p^2$)	0.69
Angularity	($p^2/4\pi A$)	1.45
Aspect ratio	(Major/minor axis)	1.33
Roundness	($p/4\pi A$)	0.34

underneath a shallow footing or in a shear box; winter sand is well-graded, angular sand.

Direct shear testing was also performed on the winter sand in a 304.8 mm square direct shear box at the same densities used for the footing tests. A large shear box was used because ASTM D 3080-90, Standard Test Method for *Direct Shear Tests of Soils under Consolidated Drained Conditions* (ASTM 1998), requires a minimum specimen thickness of six times the maximum particle diameter and a minimum specimen width of ten times the maximum particle diameter in determining what size shear box should be used for testing sands. The minimum specimen width to thickness ratio should be 2:1. The confining stresses used to determine the friction angle ranged from 35 to 250 kPa. The friction angles were calculated at 10% of the box width. The results of the shear tests provided friction angles of 40.8° at $D_r=24\%$, 44.5° at $D_r=57\%$, and $\phi=46.0^\circ$ at $D_r=87\%$.

Model Footing Tests

Model footing tests were performed in a 0.762 m \times 0.762 m \times 0.305 m steel box with a concrete base. All tests were performed under saturated conditions with the footing resting on the sand surface ($D_f=0$). The dimensions of the square and circular model footings used were 0.102 m. The sand was placed in 0.05 m lifts and spread by hand until level. A 0.15 m \times 0.15 m square steel hand tamper was used to compact the sand to the target relative density. The target densities in this study were $D_r=24$, 57, and 87%. The steel model footings were given a rough base and were loaded at a constant rate of 0.001 cm/s until a settlement of 0.1 B occurred. The ultimate bearing capacity was defined as the bearing stress producing a relative settlement, s , of $s/B=0.1$ and the bearing capacity factor, N_y^* , was backcalculated from the load at failure for both square and circular footings.

This study used the 0.1 B method, which takes the ultimate capacity at a settlement of 10% of the footing width. This method of defining the ultimate bearing capacity has previously been used (e.g., Lutenegeger and Adams 1998). Although this method is arbitrary, it: (1) is convenient and easy to remember; (2) may actually be close to the average soil strain at failure; and (3) forces a fixed value at q_{ult} .

Large Model Footing Tests

Large model footing tests were performed in a 2.44 m by 2.44 m \times 1.22 m test pit with walls and floors constructed of reinforced concrete and the loading frame constructed of steel. The walls were 0.305 m in thickness. All tests were performed under saturated conditions with the footing resting on the sand surface ($D_f=0$). The dimensions of the large model footings used were 0.152, 0.305, and 0.457 m. Square footings were tested at all three relative densities ($D_r=24$, 57, and 87%), while the circular footings were tested only at the highest relative density ($D_r=87\%$). The footings were incrementally loaded with a hydraulic jack and data were recorded using a load cell connected to a strain gauge box. Readings of the load and displacement were taken at 1, 3, 5, 7, 15, and 20 min or until movement could not be detected. The application of the incremental loads continued until a total footing settlement of at least 0.1 B .

Results

Model Footing Tests

Typical load curves for 0.102 m square model footings with a relative density equal to 87% are shown in Fig. 1. The s - q load

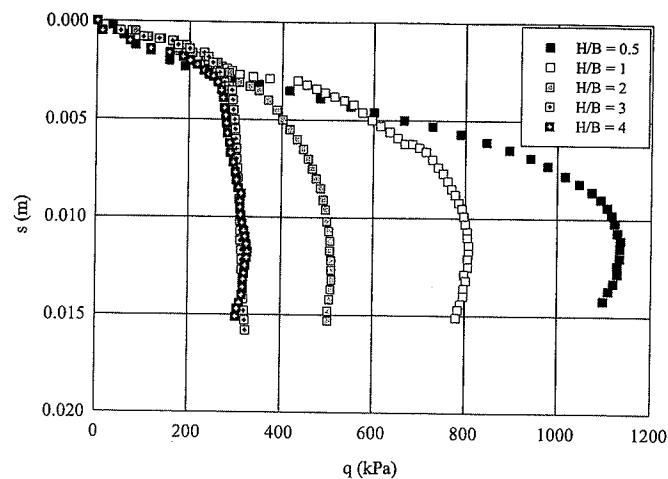


Fig. 1. Load-displacement curves for square 0.102 m model scale footing tests on dense ($D_r=87\%$) winter sand at varying H/B values

curves for the tests performed at the relative densities of 24 and 57% are similar. q_{ult} was taken at 10% of the footing width, in this case at $s=0.01$ m. Table 3 presents results of the ultimate bearing capacity for the model footing tests. The ultimate capacity, q_{ult} , results show that the square footings have a higher bearing capacity than circular footings at each density. This is consistent with Terzaghi's (1943) bearing capacity equations which indicate that a square footing will have a bearing capacity approximately $0.8/0.6=1.33$ larger than a circular footing of the same width. In this study, the ultimate bearing capacity of a square footing ranged between 1 (equal) and 1.33 times greater than the circular footing with a mean value of 1.25 times greater.

The values of N_y^* were backcalculated for each test assuming Terzaghi's (1943) definition of shape factors on an infinite layer, because the q_{ult} results from this study showed that there actually was bearing capacity differences between square and circular foundations.

Table 3. Model Footing Test Results ($B=0.102$ m)

D_r (%)	Friction angle (degrees)	Square q_{ult}^a (kPa)	Square		Circular	
			H/B	N_y^* (kPa)	q_{ult}^a (kPa)	N_y^* (kPa)
24	40.8	140	4	442	120	378
			3	473	125	394
			2	946	250	788
			1	1,577	420	1,325
			0.5	4,021	650	3,075
57	44.5	225	4	710	180	568
			3	694	180	568
			2	1,261	325	1,025
			1	2,075	500	1,660
			0.5	5,913	800	4,730
87	46.0	325	4	905	245	682
			3	905	245	682
			2	1,392	460	1,280
			1	2,344	620	1,817
			0.5	6,263	950	4,958

^a q_{ult} defined as q at $s/B=0.10$.

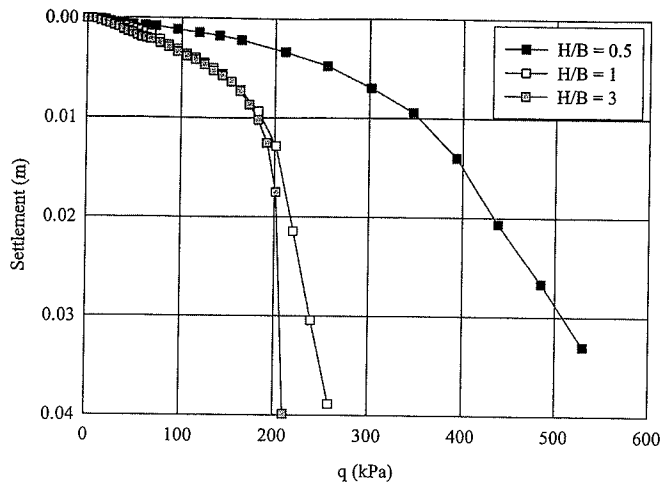


Fig. 2. Load-displacement curves for 0.305 m footing tests on dense winter sand at varying H/B values

Large Model Footing Tests

Typical load curves for 0.305 m square footings with a relative density equal to 87% are shown in Fig. 2. The $s-q$ load curves for the tests performed at the relative densities of 24 and 57% are similar. Square footing bearing capacity was typically higher than the bearing capacity of the circular footings at the same H/B values with a range of 0.85 (lower)–1.9 times higher. Table 4 presents results of the ultimate bearing capacity and backcalculated values of N_y^* for the large model footing tests.

Comparison of Test Results

Combined results of the model footings tests are presented in Fig. 3. The results show that for the 0.102 and 0.152 m footings,

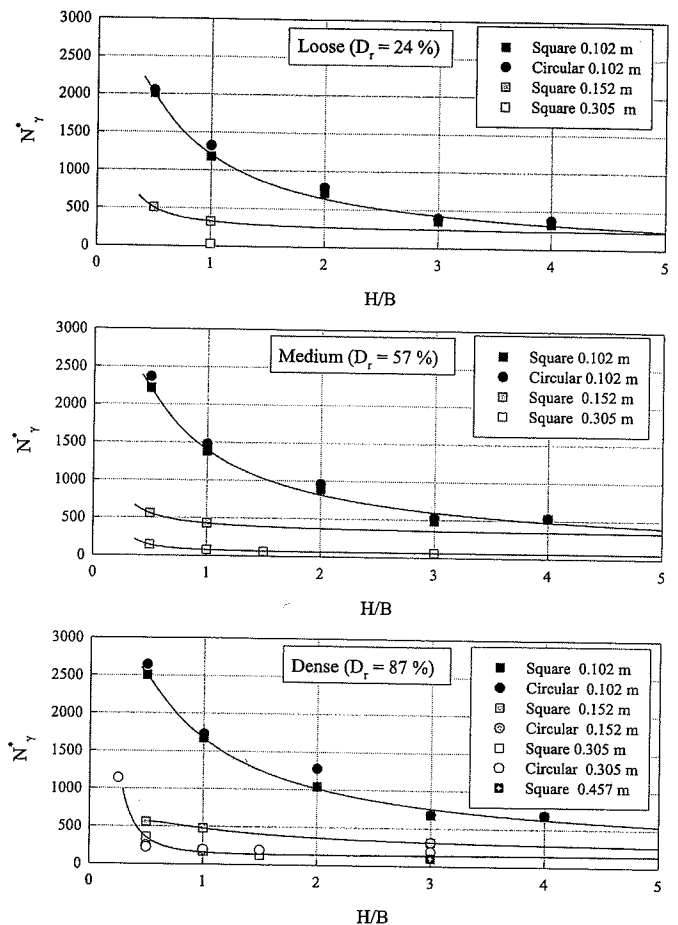


Fig. 3. Influence of H/B and footing width, B , on N_y^* for three relative densities

Table 4. Large Model Footing Test Results

D_r (%)	Square		Circular		
	H/B	B (m)	q_{ult} (kPa)	N_y^* (kPa)	
24	1	0.152	208	328	
	0.5	0.152	320	505	
	1	0.305	42	33	
57	1	0.152	290	429	
	0.5	0.152	378	559	
	3	0.305	83 ^a	62	
	1.5	0.305	82	61	
	1	0.305	110	81	
87	0.5	0.305	190	140	
	3	0.152	225	313	
	1	0.152	342	476	
	0.5	0.152	403	561	
	3	0.305	207	144	
	3	0.457	217	101	
	1.5	0.305	180	125	
	1	0.305	240	167	
0.5	0.305	512	356		
0.25	0.305	—	—	1,230	1,141

^aAverage of two tests.

^bAverage of three tests.

N_y^* values decrease with increasing H/B values becoming constant somewhere between $H/B=3$ and 4. These tests show greater H/B influence than those previously presented in the literature, which generally show that a constant value is obtained between $H/B=1.5$ and 2. The results of the 0.305 m footings show that while there is a decrease in N_y^* with increasing H/B values, the depth of influence is much less than that of the smaller footings, which may be related to differences in the mode of failure. The N_y^* values become constant at a H/B value of between 1 and 1.5, which is more consistent with previous results.

The results presented in Fig. 3 also show that N_y^* is not only dependent on H/B and D_r , but it is dependent on the footing width, B , for the same relative density, D_r , and for the same H/B values. The smaller 0.102 m footings gave higher N_y^* values than the 0.305 m footing for each of the three densities for each H/B . For all tests performed at an $H/B=1$, the smaller footing always has a higher N_y^* value than the larger footing and increases according to increasing density. In the densest state, at H/B of 3, the N_y^* value is shown to decrease with increasing footing size (0.102 m > 0.152 m > 0.305 m > 0.457 m). This phenomenon is most likely true for all H/B values and all densities. This dependence of N_y^* on footing width has been noted by others for footings resting on an infinite layer (DeBeer 1965; Hettler and Gudehus 1988; Ueno et al. 1998, 2001; Zhu et al. 2001).

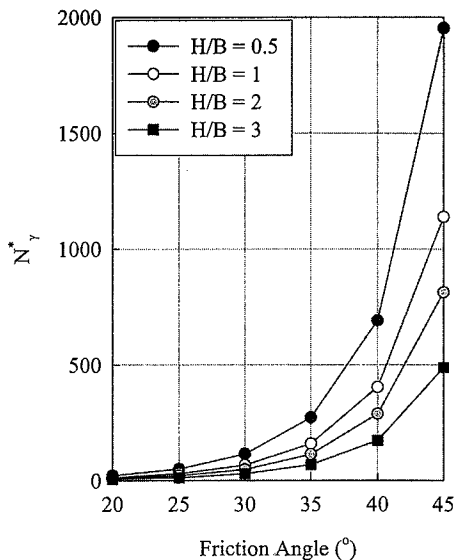


Fig. 4. Proposed design chart for modification of bearing capacity factor N_{γ}^* as function of H/B and ϕ

In this study, it was found that the depth influence extended to $H/B=3$ for footings resting on well-graded sand. Therefore, it is suggested that the previously reported modifications to both s_{γ}^* and N_{γ}^* be extended to encompass the depth influence of a footing on dense well-graded sand. This is a larger range than was first suggested by Mandel and Salencon (1972), who presented data on strip footings that showed for $H/B \geq 1$, $N_{\gamma}^* = N_{\gamma}$. In this study, it was seen that $N_{\gamma}^* = N_{\gamma}$ at $H/B \geq 3$.

Instead of modifying two parameters, s_{γ}^* and N_{γ}^* for the effects of finite layering, this study proposes using the shape factors first presented by Terzaghi (square=0.8 and circular=0.6) to account for the differences in bearing capacity due to footing shape and then modifying N_{γ}^* to account for finite layering up to $H/B \leq 3$. The results of this study show that square footings have higher bearing capacities than circular footings at all H/B values. Therefore, Meyerhof's (1974) suggestion that both square and circular footings have the same shape factor and are only affected by the rigid layers from Eq. (2) is incorrect because shape does affect bearing capacity at all H/B . A design chart for N_{γ}^* as a function of H/B and ϕ' was generated from the results of this study, showing that the layer influence H/B should extend to $H/B \leq 3$ (Fig. 4). This design chart was generated using the results of the footing tests on the densest material ($D_r=87\%$) since footings in the field will generally be built on dense, well-graded material. In order to predict the ultimate bearing capacity of a footing on a finite layer, first the appropriate shape factor ($s_{\gamma}=0.8$ square and 0.6 circular) would be chosen and then the appropriate N_{γ}^* would be chosen from Fig. 4 and used in Eq. (3) to calculate the ultimate bearing capacity.

In addition to enlarging the range of H/B values where N_{γ}^* must be modified to adjust for the influence of a rigid layer, N_{γ}^* must also be modified to adjust for the scale effect observed between N_{γ}^* and footing width, B for $B < 0.457$ m. Mandel and Salencon's (1972) modification to the bearing capacity factor as a function of H/B and friction angle did not take into consideration the scale effect seen with different size footings and N_{γ}^* , as was shown in this study. At this time, it is unclear how to adjust the design values of the modified bearing capacity factor, N_{γ}^* , for the observed scale effect, however from the results of this study it is

obvious that the modified bearing capacity factor, N_{γ}^* , should be adjusted not only for H/B and ϕ , but for footing width, B , when $B < 0.457$ m.

Conclusions

Results of the model footing tests show that the modified bearing capacity factor, N_{γ}^* , is dependent on relative density, D_r , H/B , and footing width, B . The tests indicate that N_{γ}^* decreases as footing size, B , and H/B increase and N_{γ}^* increases as relative density, D_r , increases.

From the results of this study, it can be seen that the modification of the shape factor, s_{γ}^* , should account for shape. Square footings show a higher bearing capacity than the circular footings of the same size (mean $q_{ult \text{ square}}/q_{ult \text{ circular}}=1.33$), and both square and circular footings show higher ultimate bearing capacities for H/B values ≤ 3 .

It was observed that the modification of the bearing capacity factor, N_{γ}^* , should extend to $H/B \leq 3$, for circular and square footings. This is a larger range than has previously been suggested based on results obtained from model strip footings which showed that for $H/B \geq 1$, $N_{\gamma}^* = N_{\gamma}$. In this study, it was seen that $N_{\gamma}^* = N_{\gamma}$ at $H/B \geq 3$. A design chart for the modified bearing capacity based on H/B and friction angle was presented, however, from the results in this study, it was seen that N_{γ}^* is not only a function of H/B and ϕ , but a function of footing width, B . This introduces the scale-effect dilemma, which has not been resolved as of yet.

References

- ASTM. (1998). *American Society for Testing and Materials annual book of ASTM standards, Vol. 04.08 Soil and Rock (I), D 420–D 4914*, West Conshohocken, Pa.
- Cooke, R. P. (1988). "Contact stress distributions beneath a rigid circular plate resting on a cohesionless mass." M.S. thesis, Clarkson Univ., Potsdam, N.Y.
- DeBeer, E. E. (1965). "The scale effect on the phenomenon of progressive rupture in cohesionless soils." *Proc., 6th Int. Conf. on Soil Mechanics and Foundation Engineering*, Vol. 2, No. 3–6, 13–17.
- Hanna, A. M. (1981). "Experimental study on footings in layered soil." *J. Geotech. Engrg. Div.*, 107(8), 1113–1127.
- Hettler, A., and Gudehus, G. (1988). "Influence of the foundation width on the bearing capacity factor." *Soils Found.*, 28(4), 81–92.
- Lutenegger, A. J., and Adams, M. T. (1998). "Bearing capacity of footings on compacted sand." *Proc., 4th Int. Conf. on Case Histories in Geotechnical Engineering*, 1216–1224.
- Mandel, J., and Salencon, J. (1972). "Force portante d'un sol sur une assise rigide (Etude Theorique)." *Geotechnique*, 22(1), 79–93.
- Meyerhof, G. G. (1974). "Ultimate bearing capacity of footings on sand layer overlying clay." *Can. Geotech. J.*, 11, 223–229.
- Narahari, D. R., and Singh, A. (1964). "Effect of stratification on the bearing capacity of footings on sand." *J. Indian Nat. Soc. Soil Mech. Found. Eng.*, 4, 228–237.
- Pfeifle, T. W., and Das, B. M. (1979). "Model tests for bearing capacity in sand." *J. Geotech. Engrg. Div.*, 105(9), 1112–1116.
- Siraj-Eldine, K., and Bottero, A. (1987). "Etude experimentale de la capacite portante d'une couche de sol pulverulent d'epaisseur limitee." *Can. Geotech. J.*, 24, 242–251.
- Terzaghi, K. (1943). "Bearing capacity." *Theoretical soil mechanics*, Chap. 8, 118–143.

- Tournier, J. P., and Milovic, D. M. (1977). "Etude experimentale de la capacite portante d'une couche compressible d'epaisseur limitee." *Geotechnique*, 27(2), 111-123.
- Ueno, K., Miura, K., Kusakabe, O., and Nishimura, M. (2001). "Reappraisal of size effect of bearing capacity from plastic solution." *J. Geotech. Geoenviron. Eng.*, 127(3), 275-281.
- Ueno, K., Miura, K., and Maeda, Y. (1998). "Prediction of ultimate bearing capacity of surface footings with regard to size effects." *Soils Found.*, 38(3), 165-178.
- Zhu, F., Clark, J. I., and Phillips, R. (2001). "Scale effect of strip and circular footings resting on a dense sand." *J. Geotech. Geoenviron. Eng.*, 127(7), 613-621.